NEXT-GENERATION TRANSIT SURVEY SECOND DATA RELEASE DOCUMENT

Data release description and supplemental information for the second public data release from the Next-Generation Transit Survey (NGTS)

NGTS Consortium

July 20, 2020

http://ngtransits.org

Contents

Acronyms

CCD Charged-Coupled Device

FOV Field of View

FWHM Full Width at Half Maximum

MCMC Markov chain Monte-Carlo

NGTS The Next-Generation Transit Survey

PSF Point-Spread Function

QE Quantum Efficiency

RMS Root Mean Square

SNR Signal-to-Noise Ratio

VLT Very Large Telescope

Abstract

The Next-Generation Transit Survey (NGTS) is a ground-based exoplanet survey designed to detect and study Neptune and super-Earth sized planets around bright host stars using the transit method. The project is described by Wheatley et al. (2018) and the project website is `http://ngtransits.org`.

The NGTS facility consists of 12 robotic telescopes situated at the European Southern Observatory (ESO) site in Paranal, Chile. Each 20-cm, f/2.8 telescope has a field-of-view of $2.8° \times 2.8°$ and is equipped with a custom NGTS filter and an Andor iKon-L 936 camera, which uses a deep-depletion CCD42-40 back-illuminated CCD sensor.

During commissioning and the first two years of science observations, spanning 21-Sep-2015 to 01-Apr-2018, NGTS observed 72 fields. A total of 110 982 662 788 (1.1×10^{11}) photometric measurements were made of 629 421 targets from 12 850 709 images, taken at a cadence of 13 seconds. Each field was imaged between 64 000 and 250 000 times. For each field, we have released an example science image, a source list with cross-matched identifiers from other surveys, a stacked frame from which the source list was generated, and the detrended source lightcurves produced by aperture photometry. These data constitute NGTS Data Release 2 (DR2).
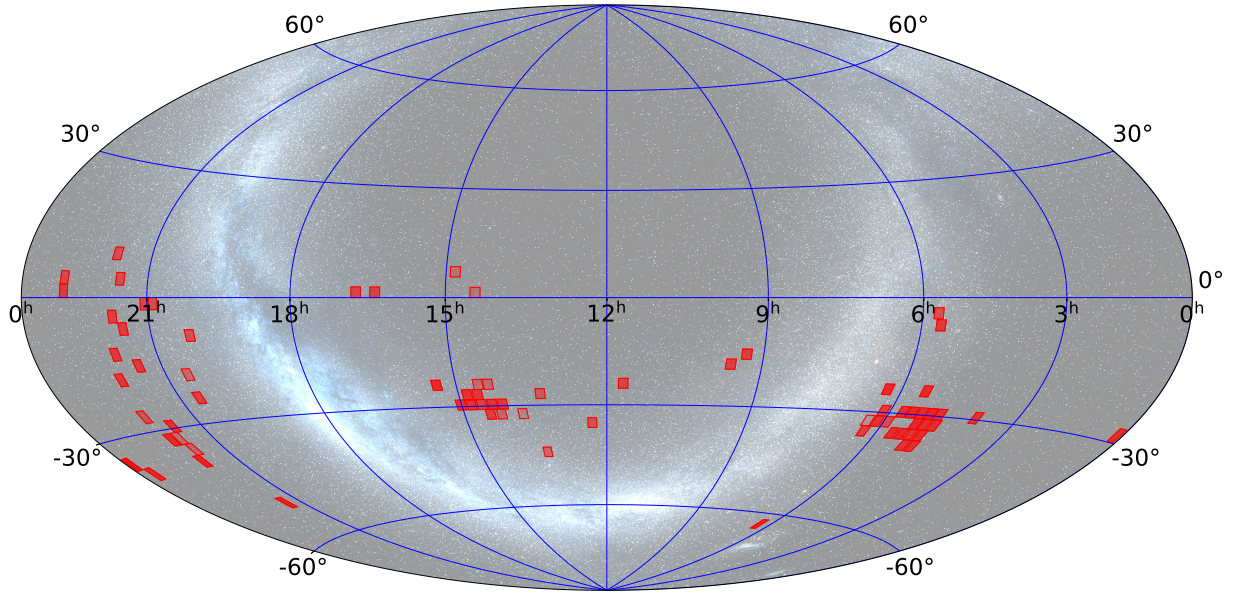
Figure 1: The sky coverage of NGTS DR2. The intensity of the shading of each field is proportional to the number of images of that field.

1 Overview of Observations

A total of 72 fields measuring $2.8 \times 2.8°$ are included in the second data release. The sky coverage of NGTS DR2 is shown in Figure 1. These fields were observed over the course of two and a half years spanning the period 21-Sep-2015 to 01-Apr-2018. Fields were included in NGTS DR2 if the final date of observation was before 01-Apr-2018, the two-year cut-off for the data release marked from the start of routine survey operation on 01-Apr-2016. Fields which were not completed during the second year will be included in the next data release.

The individual object lightcurves were sampled at 13-second cadence, with a 10 second exposure time, and contain between $64\,000$ and $250\,000$ data points depending on the field. Observations were conducted by the 12 NGTS telescopes, which are described in full by Wheatley et al. (2018). Each telescope is fitted with a custom NGTS filter with a bandpass of 520–890 nm, which increases sensitivity to late-K and early-M stars. Figure 2 shows the CCD QE, filter transmission curve and the expected throughput of the telescope.

Each telescope followed one field from when it rose above an elevation of 30° until when it set below 30°. Once a field had set, another was picked up for the remainder of the night. Fields were chosen to minimize idle time, with each telescope typically observing 2 fields per night. Fields were selected from a discrete mesh of 5,307 mesh centers, and were chosen to maximize expected planetary yield, based on: the density of stars, expected number of dwarf stars, ecliptic latitude and the presence of bright stars or other extended objects in the field of view (FOV).
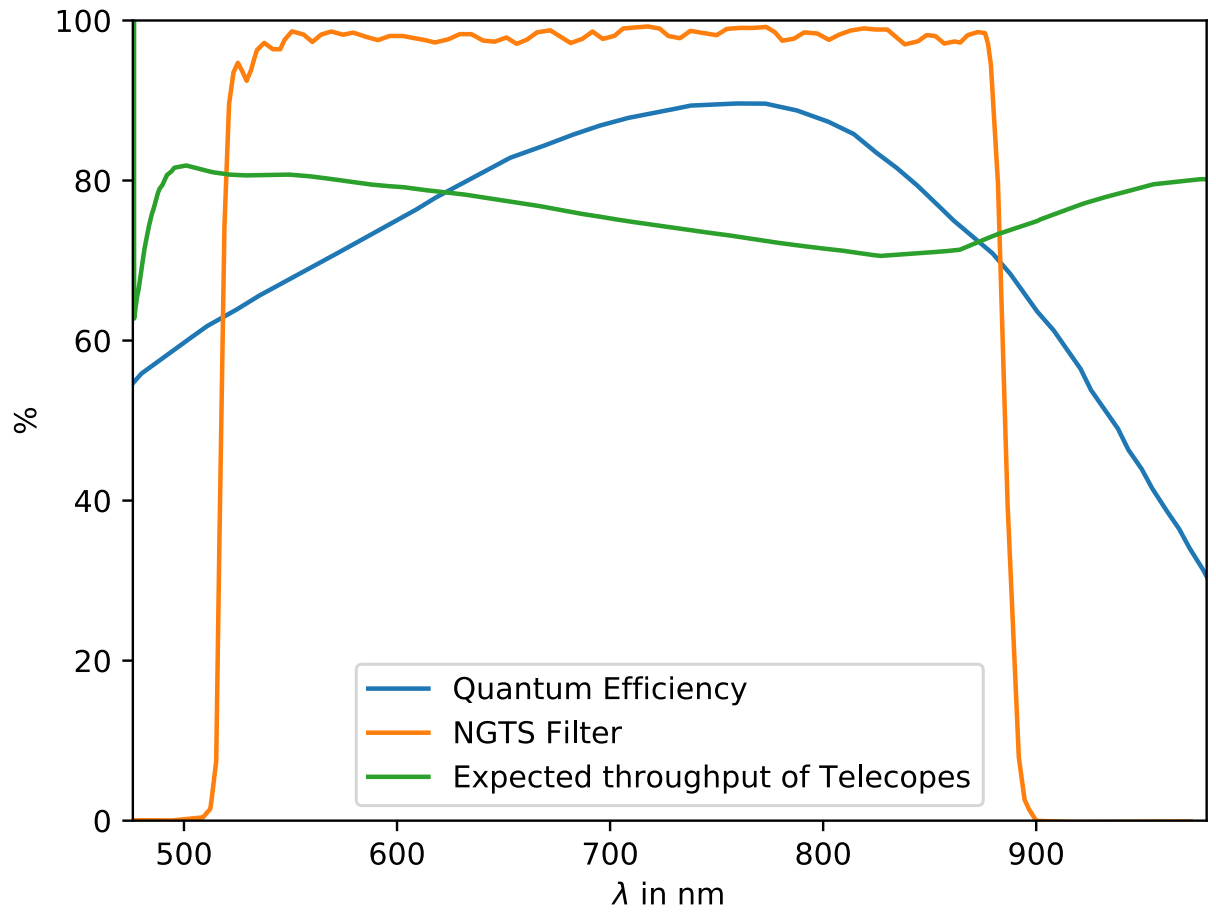
4

Figure 2: A plot showing the transmission curve of the custom NGTS filter, the measured QE for the CCD chip and the telescope throughput. This plot is from Wheatley et al. (2018)

Table 1: Summary of the data products released for each NGTS field, where {FIELD} denotes the field name. The example science frame is a high-quality frame taken under good conditions at low airmass. The dithered stack frame is a super-sampled image, constructed from a series images with dithered pointing, from which the source catalogue is derived. The source and lightcurve catalogues are, respectively, the source list and the photometric lightcurves. The lightcurves for each field are separated on a 5 by 5 equal-sized grid and each tile is assigned a letter from A to Y. This is denoted by {LETTER} in the naming convention.

Data Product	PRODCATG Keyword	Naming Convention
Example Science Frame	ANCILLARY.IMAGE	AG_REFERENCE_{FIELD}.fits
Dithered Stack	SCIENCE.IMAGE	DITHERED_STACK_{FIELD}.fits
Source Catalogue	SCIENCE.CATALOGTILE	SOURCE_CATALOGUE_{FIELD}.fits
Lightcurve Catalogue	SCIENCE.CATALOGTILE	FLUX_{FIELD}{LETTER}.fits

The lightcurves were reduced via the usual procedure, using bias, dark and sky flat-field frames taken over the course of observations. Bias and dark frames were taken at dawn after the telescopes had been stowed and the enclosure had been closed. Flat-field frames were taken at dawn and dusk, when the weather was clear, and were carefully processed to remove clouds and stars.

2 Previous Releases

Since the first NGTS data release, NGTS DR1, we made improvements to our flat fielding, source detection and detrending techniques. Therefore we reprocessed all existing data and, for uniformity, NGTS DR2 includes a new release of the 24 fields of NGTS DR1.

3 Release Content

3.1 Overview

NGTS DR2 consists of 4 data products as 28 separate files for each observed field. These data products are summarised in Table 1, and consist of: an example high-quality science image; a super-sampled stacked image; a source catalogue generated from the stacked image; and the lightcurves of the objects in the source catalogue. For technical reasons, each field has been split into an equal 5x5 grid and the lightcurves are provided as 25 separate files. In total the data release consists of 3.98 TB of data across 2018 files.

3.2 Image Data Products

Each stacked image was constructed from 150 images, which were taken using a dithered motion with a random offset of around 6 pixels (30 arcsec) from the nominal field centre. These frames were taken at a low airmass during dark time. The images were reduced, aligned to sub-pixel precision using the same algorithm used by the NGTS autoguider (Wheatley et al., 2018), then accumulated into a stacked image that is super-sampled by a factor 8 along each axis. This dithering and super-sampling was performed to mitigate the relatively under-sampled PSF, allowing a more accurate source detection, centroiding and astrometry for the source catalogue. This super-sampling allows better disambiguation of blended sources that are resolvable with NGTS.

The second image provided for each field is an example of a typical science frame. The image selected was taken in good conditions and was used as the autoguider reference image.

3.3 Source Catalogue

The source catalogue was constructed from the stacked frame described in Section 3.2. The catalogue was constructed using the IMCORE tool (Irwin et al., 2004) from the CASUTOOLS software package[1]. The source detection finds targets down to $I_{\mathrm{mag}} = 19$, but for practical purposes, as well as to focus on the primary scientific aim of the survey, we set the faint limit of the source catalogue as $I_{\mathrm{mag}} = 16$. Lightcurves were only generated for the sources in the catalogue, and so any sources fainter than $I_{\mathrm{mag}} = 16$ magnitude are not included in the data release.

Each source was cross-matched with the following catalogues: the AAVSO Photometric All-Sky Survey (Henden and Munari, 2014), GAIA DR2 (Gaia Collaboration et al., 2018), 2MASS (Skrutskie et al., 2006), UCAC4 (Zacharias et al., 2013), ALLWISE (Cutri and et al., 2014), RAVE (Kunder et al., 2017) and GALEX (Martin et al., 2005). The cross-matched identifiers are provided in the source catalogue to enable easy identification of targets of interest.

Spurious sources were removed from the catalogue by checking for multiple detections within the spatial resolution of NGTS. This is further discussed in Section 5.

Information from the source detection, astrometry and catalogue cross-matching is combined into the NGTS DR2 source catalogue. Each entry in the catalogue is for a unique source and is structured as follows:

- **SOURCE_ID**: Unique source identifier constructed from the RA and DEC from the astrometric fit

- **RA_NGTS [deg]**: RA coordinate for the source.

- **DEC_NGTS [deg]**: DEC coordinate for the source.

---

[1]http://casu.ast.cam.ac.uk/surveys-projects/software-release

- **NGTS_MAG [mag]**: Magnitude of the source in the NGTS passband (see Fig. 2).

- **REF_FLUX [ADU/s]**: Reference flux used to calculate the NGTS magnitude, taken from the dithered stacked frame.

- **FLUX_MEAN [ADU/s]**: Mean flux for the source.

- **FLUX_RMS [ADU/s]**: RMS variability for the source.

- **CCDX, CCDY [pixel]**: Position of the source as measured on the dithered stack frame for that field.

- **NPTS_TOTAL**: Total number of data points acquired for the source including null and clipped data points.

- **NPTS**: Number of good data points for the source lightcurve.

- **NPTS_CLIPPED**: Number of data points excluded by a 7-sigma clip of the lightcurve.

- **NPTS_NOT_NULL**: Number of data points which are not null.

- **FLAG_CNT0-4**: A value counting the total number of times each of the five data quality flags has been triggered for the source. See Section 3.4.

- **Cross-matched identifiers**: The identifiers are provided from a cross-match with the following surveys: GAIA DR2, 2MASS, PPMXL, UCAC4, NED, GALEX, WISE, RAVE, DENIS and USNO-B1.0.

- **NPTS_CLIPPED**, **FLAG_CNT_1** and **NED_ID** are placeholder columns with no information.

Table 2: Summary of the fields in NGTS DR2. The table contains the field name, unique camera identifier, number of sources, number of science frames, and the start and end dates of the observations.

Field	Camera ID	Sources	Images	Start Date	End Date
NG0004−2950	812	3574	203351	2017-05-06	2017-11-18
NG0353−3056	813	4161	191716	2017-08-15	2018-03-17
NG0442−3345	801	5059	202904	2017-08-15	2018-03-17
NG0445−3056	811	5466	204178	2017-08-15	2018-03-22
NG0448−3922	808	5516	199434	2017-08-15	2018-03-17
NG0450−3633	804	5418	205412	2017-08-15	2018-03-17
NG0456−3345	803	5637	197896	2017-08-15	2018-03-17
NG0458−3056	807	5881	214878	2017-08-15	2018-03-22
NG0502−3922	809	6026	191564	2017-08-15	2018-03-17
NG0504−3633	806	6137	197822	2017-08-15	2018-03-17
NG0509−3345	810	6498	211325	2016-08-07	2017-04-25
NG0511−3056	810	6118	203460	2017-08-16	2018-03-27
NG0518−3633	813	7056	215040	2016-08-06	2017-04-25

NG0522−2518	802	7554	216839	2015-09-21	2016-05-03
NG0524−3056	803	7485	214918	2016-08-06	2017-05-01
NG0531−0826	806	10472	197151	2015-09-23	2016-04-20
NG0532−3633	809	7386	211070	2016-08-06	2017-05-01
NG0535−0523	802	8957	163821	2017-08-16	2018-03-17
NG0537−3056	801	8078	209550	2016-08-06	2017-05-02
NG0549−3345	805	8924	155909	2016-08-06	2017-05-01
NG0603−3056	811	12428	190696	2016-08-06	2017-05-05
NG0603−3345	804	10246	203129	2016-08-06	2017-05-05
NG0612−2518	805	13430	221621	2015-09-21	2016-05-14
NG0613−3633	812	11394	191374	2016-08-18	2017-05-18
NG0616−3345	807	12554	63618	2017-01-27	2016-09-02
NG0618−6441	801	11479	235266	2015-09-21	2016-05-24
NG0914−1652	802	10984	184572	2016-10-07	2017-06-21
NG0931−1941	806	11024	186107	2016-10-07	2017-06-21
NG1135−2518	809	6597	169344	2015-11-26	2016-03-07
NG1213−3633	810	10690	150489	2015-11-28	2016-08-04
NG1315−2807	812	8207	134312	2016-01-05	2016-08-31
NG1318−4500	811	20194	140820	2015-12-17	2016-08-31
NG1340−3345	808	11427	78516	2016-04-18	2016-08-31
NG1403−3056	813	13375	187825	2017-01-01	2017-08-14
NG1407−3345	810	12284	122543	2017-01-01	2017-05-07
NG1416−2518	806	8569	105573	2016-01-05	2016-09-16
NG1416−3056	809	11161	200237	2017-01-01	2017-08-20
NG1421+0000	805	4341	91077	2016-01-05	2016-08-31
NG1421−3345	805	13099	190589	2017-01-25	2017-08-24
NG1428−2518	802	9030	108918	2016-01-05	2016-09-19
NG1429−3056	803	11419	174684	2017-01-01	2017-08-24
NG1431−2807	807	10419	194270	2017-01-27	2017-08-24
NG1442−3056	801	12096	203788	2017-01-01	2017-08-24
NG1444+0537	801	4226	87151	2016-01-13	2016-09-03
NG1444−2807	804	10962	204148	2017-01-25	2017-08-25
NG1455−3056	811	13824	206266	2017-01-25	2017-08-25
NG1518−2518	812	15379	220897	2017-01-25	2017-09-21
NG1615+0000	802	8371	174471	2017-03-04	2017-09-21
NG1637+0000	806	11378	174384	2017-03-04	2017-09-21
NG2004−1028	813	22583	164918	2017-04-25	2017-11-14
NG2025−1941	813	12901	119157	2016-04-20	2016-11-30
NG2028−2518	802	10962	180854	2015-09-21	2016-12-06
NG2047−0248	810	12872	161769	2016-04-20	2016-12-01
NG2058−0248	803	10805	170323	2016-04-20	2016-12-01
NG2121−5148	808	7058	228184	2017-04-20	2017-11-25
NG2126−1652	804	6967	181379	2016-04-20	2016-12-15
NG2131−0826	807	7350	181465	2017-04-22	2017-11-22

NG2132+0248	805	8623	158453	2016-04-20	2016-12-02
NG2137−3056	801	5782	199063	2017-04-22	2017-11-22
NG2141−3633	810	5719	121377	2017-04-21	2017-12-08
NG2142+0826	801	9228	156463	2016-04-20	2016-12-02
NG2143−0537	804	7317	177485	2017-04-22	2017-11-22
NG2145−3345	808	5739	94332	2016-04-20	2016-09-02
NG2150−3922	812	5750	224159	2016-04-20	2016-12-27
NG2152−1403	811	5784	181260	2016-04-20	2016-12-21
NG2158−3345	809	4992	210818	2017-04-22	2017-11-22
NG2201−1941	811	5489	186609	2017-04-22	2017-11-22
NG2206−2807	803	5139	140395	2017-04-22	2017-11-22
NG2251+0000	802	4425	179765	2017-05-07	2017-12-14
NG2251+0248	806	4945	160487	2017-05-07	2017-11-24
NG2331−3922	806	3580	216979	2016-05-03	2017-01-10
NG2346−3633	802	3421	250092	2016-05-03	2017-01-25

3.4 Lightcurves

The NGTS DR2 consists of 72 fields of data, each covering an area of $2.8 \times 2.8°$. A complete list of fields is included in Table 2. The fields have between $3\,000$ and $23\,000$ individual sources, each of which has a lightcurve measured at a cadence of 13 seconds, covering the duration over which the field was observed.

The lightcurves were produced using the NGTS pipeline, as described in Section 5, and were de-trended using the SYSREM algorithm (Tamuz, Mazeh, and Zucker, 2005), which removes systematic trends found in multiple stars. SYSREM is a dimensionality reduction algorithm, which reduces to Principle Component Analysis (Pearson, 1901) when the error on each measurement is assumed to be zero.

A customised version of SYSREM was used for the NGTS data, based on the algorithm used by the WASP project (Collier Cameron et al., 2006). An initial coarse decorrelation removes the most significant trend in the data, which is due to the time-dependent atmospheric extinction as the field rises and sets throughout the night. Four further common trends are then removed from the data. In addition to removing systematic trends from the data, SYSREM also produces a per-image down-weight based on the intra-image variance of the instantaneous flux of each of the ensemble of stars about their respective global mean fluxes. This down-weight is propagated through to the error, using

$$\sigma_{i,new} = f_i \sqrt{(\sigma_i/f_i)^2 + \sigma_t^2}, \qquad (1)$$

where f_i is the flux measurement and σ_i its formal photometric error, and σ_t is the additional down-weight for the image (Collier Cameron et al., 2006).

The final SYSREM-corrected lightcurves are provided in the form of a catalogue. Every entry in the catalogue is a single photometric data point and contains the following information:

- **SOURCE_ID**: a unique identifier for each source constructed from it's RA and DEC.
- **HJD [days]**: The time at which the measurement was taken, converted into HJD (UTC).
- **SYSFLUX [ADU/s]**: The SYSREM-corrected flux measurement.
- **FLUX_ERROR [ADU/s]**: The SYSREM down-weighted error in the flux measurement.
- **FLAG**: The NGTS data quality flag.

Erroneous flux measurements produced by the pipeline were either set to 'not a number' (NaN) or to zero. Additionally, the NGTS flagging system is used to identify data points which are statistical outliers, or which may have been affected by bright stars, airplanes crossing the FOV or other contaminants such as the lasers used by the adaptive optics system of VLT UT4. Each flag consists of a single bit in an 8-bit integer which encodes a unique description of why the data point may have been flagged. The full list of flags can be found in Table 3.

4   Release Notes

NGTS is a ground-based exoplanet survey designed to detect and study Neptune-size and super-Earth-size planets around bright host stars using the transit method. A detailed description of the project can be found in Wheatley et al. (2018). NGTS observes fields in a custom bandpass from 520–890 nm (Figure 2), which increases sensitivity to late-K and early-M stars. NGTS achieves better than 1 mmag noise for most stars of $I_{\mathrm{mag}} < 12$ in one hour of exposure time (Figure 3). Each NGTS image is calibrated using high quality bias and sky flat-field frames taken both before and after the science observations. Source detection is performed on a stack of dithered frames, designed to improve the accuracy of the detection. Each image is solved astrometrically for accurate placement of the apertures used to perform photometry. The lightcurves are detrended using a custom version of the SYSREM algorithm (Tamuz, Mazeh, and Zucker, 2005; Collier Cameron et al., 2006).

5   Data Reduction and Calibration

The NGTS pipeline takes raw images, both science and calibration, and produces high-quality detrended lightcurves for each detected source. The full structure of the pipeline is
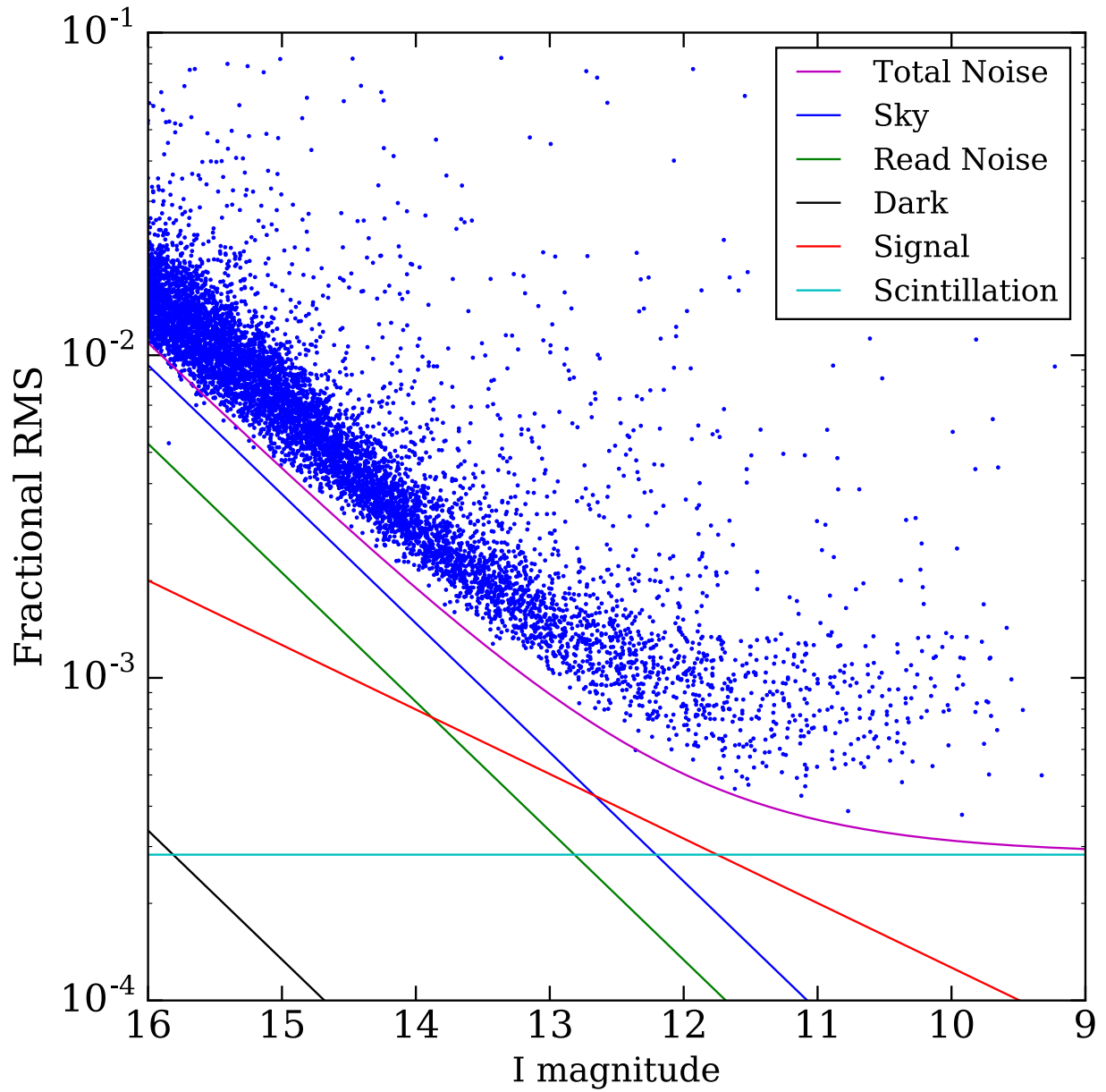
Figure 3: A comparison of the measured fractional RMS noise level of a single NGTS field compared with a theoretical model of the expected noise contributions. The NGTS data were detrended and binned with a bin width of 1 hour. This plot is from Wheatley et al. (2018).

Table 3: Table describing the data quality flags employed by the NGTS pipepline to screen for erroneous data points.

Flag Name	Flag Description	Bit
Saturation	The maximum ADU in the aperture exceeds a camera-specific saturation threshold	bit 0
Cosmic	Flagged if a cosmic ray has hit the CCD in the aperture	bit 1
Crossing	Aperture is intersected by a large pixel-connected region above threshold which also intersects at least two boundaries of the image (most commonly the VLT laser system).	bit 2
Outlier	The data point is found to be a $> 7\sigma$ outlier	bit 3
Spike	Aperture is intersected by a connected-pixel region that contains pixels above saturation (most commonly blooming spikes from neighbouring bright stars)	bit 4
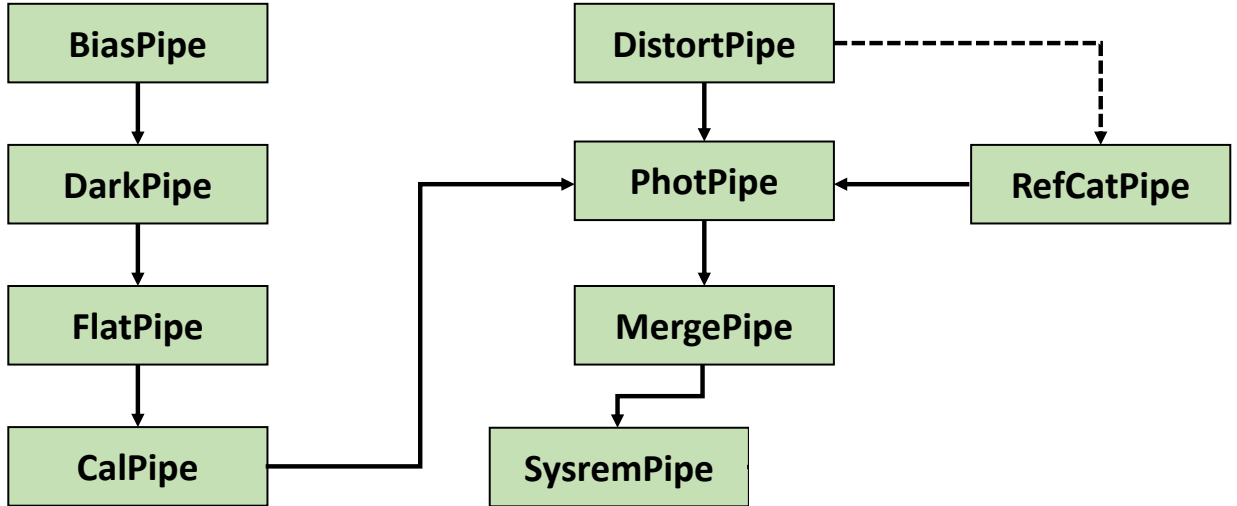
Figure 4: A schematic illustration of the NGTS photometric pipeline. Each box represents a distinct component in the NGTS pipeline and a single step in the processing of the data. BiasPipe, DarkPipe, FlatPipe and CalPipe are responsible for the production of high quality bias, dark and flat-field calibration frames. DistortPipe and RefCatPipe produce the astrometric calibration and source catalogue respectively. PhotPipe, MergePipe and SysremPipe produce the raw and then detrended lightcurves.

shown in Figure 4 as a schematic diagram. The calibration frames are processed through BiasPipe, DarkPipe and FlatPipe and then through Calpipe to produce high-quality master frames.

PhotPipe processes the science images, performing image reduction, astrometry and aperture photometry. Each science frame is trimmed to remove the overscan and then is bias and flat-field corrected in the usual way. A model of the radial distortion of the telescope is calculated once for each field using a custom MCMC code (DistortPipe). A 7th order polynomical is used with the distortion described by the 3rd, 5th and 7th order terms (Wheatley et al., 2018). The distortion is stable over time, and it is only updated when any changes are made to the telescope hardware (e.g. for replacement of camera shutters). PhotPipe solves each image astrometrically so that apertures can be placed accurately. Each image is background-subtracted by calculating an interpolated value for the background on a 64 by 64 pixel grid using a k-sigma clipped median. This improves the SNR of the background measurement while preserving some of the local structure.

MergePipe collates the raw photometry for each field into a single data product covering a full observing season, which is then passed through SysremPipe to produce the corrected lightcurves that make up the bulk of NGTS DR2. The detrending algorithm employed by SysremPipe is described in section 3.4. It is a custom version of the SYSREM algorithm (Tamuz, Mazeh, and Zucker, 2005; Collier Cameron et al., 2006).

Source Catalogue

The source detection is run using the IMCORE tool from the CASUTOOLS software package (Irwin et al., 2004). It is run on the dithered stacked frame from the field in order to better sample the stellar profile and produce more accurate source positions.

Astrometric Solution

For each science image, an astrometric solution is found in order to accurately place photometric apertures on each source. The NGTS telescopes have a non-linear radial distortion, and so a zenith polynomial projection is used (Calabretta and Greisen, 2002). The radial distortion is measured once for each field using a custom MCMC code (DistortPipe), and this only updated if telescope hardware maintenance is carried out. A 7th order polynomical is used with the distortion described by the 3rd, 5th and 7th order terms (Wheatley et al., 2018). The per image astrometric solutions account for rotation and translation, as well as shear arising from atmospheric refraction.

Photometry

NGTS photometry is performed using the IMCORE package with a 3-pixel radius, soft-edged aperture, which is placed at the source position based on the derived astrometric solution. The PSF FWHM is approximately 1.6–1.8 pixels and so less than 1% of light is lost due to the finite aperture size. The NGTS pipeline performs only relative photometry as an absolute photometric calibration is not necessary for the primary science goal of

the survey. No explicit corrections are applied to the photometric measurements due to seeing variations over time as, given the pixel scale and size of the photometric aperture used, the effects of variable seeing are minimal.

6 Data Quality

Various data quality checks are carried out automatically within the calibration steps, particularly for flat-field frames, to reject saturated frames, frames afflicted by clouds and frames containing residual stars. In addition, all master calibration frames (from CalPipe) are visually inspected for quality and checked with statistical tests.

A full astrometric calibration is performed on each autoguider reference image, including terms that describe the optical distortions. PhotPipe uses the appropriate DistortPipe parameters as an initial guess of the astrometric solution for each science image. The astrometric fitting in PhotPipe only varies the WCS parameters that encode the pointing position (including rotation), but not the distortion. The RMS error of the DistortPipe fit is recorded and if this value is above a pre-determined threshold then PhotPipe falls back on the astrometric solution from RefCatPipe, which was used during compilation of the source catalogue. Although the best result for each astrometric fit is assured, fitting is carried out on a field-by-field basis and residuals may vary by camera and by field.

During compilation of the source catalogue in RefCatPipe, contamination due to spurious objects is mitigated by cross-matching the results from the source detection with the external catalogues listed in Section 3.3. We place empirically defined limits on colour and separation to improve the accuracy of the cross-matching and screened for known variable stars and extra-galactic sources. The Gaia cross-match is used to determine whether each NGTS source is a single object or a blend that is unresolved in NGTS images. Objects fainter than 16th magnitude in the NGTS passband are cut from the catalogue, thus this is the completeness limit at the faint end. RefCatPipe outputs are manually checked for quality assurance.

The quality of the final photometry is assessed both visually and via statistical metrics, e.g. by comparing fractional RMS flux vs stellar magnitude, see Figure 3. Each flux data point has an associated data quality flag; see Section 3.4 for a full description.

7 Acknowledgements

References

Calabretta, M. R. and E. W. Greisen (Dec. 2002). "Representations of celestial coordinates in FITS". In: *A&A* 395, pp. 1077–1122. DOI: 10.1051/0004-6361:20021327. arXiv: astro-ph/0207413 [astro-ph].

Collier Cameron, A. et al. (2006). "A fast hybrid algorithm for exoplanetary transit searches". In: *Monthly Notices of the Royal Astronomical Society* 373.2, pp. 799–810. DOI: 10.1111/j.1365-2966.2006.11074.x. eprint: /oup/backfile/content_public/journal/mnras/373/2/10.1111/j.1365-2966.2006.11074.x/2/mnras0373-0799.pdf. URL: http://dx.doi.org/10.1111/j.1365-2966.2006.11074.x.

Cutri, R. M. and et al. (Jan. 2014). "VizieR Online Data Catalog: AllWISE Data Release (Cutri+ 2013)". In: *VizieR Online Data Catalog* 2328.

Gaia Collaboration et al. (Aug. 2018). "Gaia Data Release 2. Summary of the contents and survey properties". In: *A&A* 616, A1, A1. DOI: 10.1051/0004-6361/201833051. arXiv: 1804.09365 [astro-ph.GA].

Henden, A. and U. Munari (Mar. 2014). "The APASS all-sky, multi-epoch BVgri photometric survey". In: *Contributions of the Astronomical Observatory Skalnate Pleso* 43, pp. 518–522.

Irwin, Mike J. et al. (2004). *VISTA data flow system: pipeline processing for WFCAM and VISTA*. DOI: 10.1117/12.551449. URL: https://doi.org/10.1117/12.551449.

Kunder, A. et al. (Feb. 2017). "The Radial Velocity Experiment (RAVE): Fifth Data Release". In: *AJ* 153, 75, p. 75. DOI: 10.3847/1538-3881/153/2/75. arXiv: 1609.03210 [astro-ph.SR].

Martin, D. C. et al. (Jan. 2005). "The Galaxy Evolution Explorer: A Space Ultraviolet Survey Mission". In: *ApJ* 619, pp. L1–L6. DOI: 10.1086/426387. eprint: astro-ph/0411302.

Pearson, K (1901). "LIII. On lines and planes of closest fit to systems of points in space". In: *The London, Edinburgh, and Dublin Philosophical Magazine and Journal of Science* 2.11, pp. 559–572. DOI: 10.1080/14786440109462720. eprint: https://doi.org/10.1080/14786440109462720. URL: https://doi.org/10.1080/14786440109462720.

Skrutskie, M. F. et al. (Feb. 2006). "The Two Micron All Sky Survey (2MASS)". In: *AJ* 131, pp. 1163–1183. DOI: 10.1086/498708.

Tamuz, O., T. Mazeh, and S. Zucker (Feb. 2005). "Correcting systematic effects in a large set of photometric light curves". In: *mnras* 356, pp. 1466–1470. DOI: 10.1111/j.1365-2966.2004.08585.x. eprint: astro-ph/0502056.

Wheatley, P. J. et al. (Apr. 2018). "The Next Generation Transit Survey (NGTS)". In: *MNRAS* 475, pp. 4476–4493. DOI: 10.1093/mnras/stx2836. arXiv: 1710.11100 [astro-ph.EP].

Zacharias, N. et al. (Feb. 2013). "The Fourth US Naval Observatory CCD Astrograph Catalog (UCAC4)". In: *AJ* 145, 44, p. 44. DOI: 10.1088/0004-6256/145/2/44. arXiv: 1212.6182 [astro-ph.IM].